Journal of Renewable Materials

Tech Science Press

DOI: 10.32604/jrm.2021.015040

ARTICLE

Structure Design and Properties of Three-Layer Particleboard Based on High Voltage Electrostatic Field (HVEF)

Man Yuan, Lu Hong, Zehui Ju, Wenli Gu, Biqing Shu, Jianxin Cui, Xiaoning Lu* and Zhiqiang Wang*

College of Materials Science and Engineering, Nanjing Forestry University, Nanjing, 210037, China

*Corresponding Authors: Xiaoning Lu. Email: luxiaoning-nfu@126.com; Zhiqiang Wang. Email: wangzhiqiang@njfu.edu.cn

Received: 18 November 2020 Accepted: 16 December 2020

ABSTRACT

In this study, the effects of three different particle sizes of wood wastes (A = −8 + 12 mesh; B = −12 + 20 mesh; C = −20 + 30 mesh) and factory shavings (D) on the properties of particleboard were investigated. According to the test results, three-layer particleboard was designed. Particleboard face layers made with mixture of A, B, and C. The core layer made with D. The ratio of core layer to face layers is 50:50. Three-layer particleboard were fabricated with 12% urea-formaldehyde (UF) resins and three different high voltage electrostatic field intensities (0 kv, 30 kv, 60 kv). The internal bond (IB) strength, modulus of rupture (MOR), modulus of elasticity (MOE), thickness swelling (TS), and water absorption (WA) of particleboard were evaluated. The density distribution of the three-layer particleboard were examined by vertical density profiles (VDP), and the bonding mechanism and functional groups changes in the particles were analyzed by FTIR analysis. The results showed that HVEF treatment intensity play a remarkable role in properties of particleboard. The particleboard with higher electrostatic field intensities treatment has higher MOE, MOR, IB, and TS. Under HVEF treatment (60 kv), the MOR, modulus of MOE, and IB of three-layer particleboard were 23.61 N/mm^2, 2787.09 N/mm^2, and 0.86 N/mm^2, respectively. FTIR indicated that the surface activity of wood particles was increased electric field treatment.

KEYWORDS

High voltage electric field; three-layer particleboard; physical property; mechanical property

1 Introduction

As the three basic building materials, Wood products are easy to be processed into different shapes and sizes of materials, widely applied in furniture, decoration and construction industries. In recent years, timber resources are increasingly scarce, and timber supply and demand are contradictory. The efficient use of wood pellets can minimize production costs and reduce the adverse environmental impact of waste [1].

Particleboard manufactured from wood particles or other wood fiber material scraps and synthetic adhesives can be extensively used in buildings, furniture and cabinets. It can convert relatively useless, small-sized, or low-grade wood particles into useful large boards [2–3].

The mechanical, physical, and surface properties of particleboard are important indicators for evaluating its quality [4]. The development of particleboard mechanical properties depends on the type and amount of adhesive and additives, the temperature of hot pressing, the type of raw materials used, the geometry (size and shape) of the wood particles, and process parameters.

The geometry structure of wood particle has a significant effect on the properties of particleboard [5]. Long and thin particles have a bigger surface, which provides a larger contact area for the connection between the adhesives and the particles [6]. Small and thin particles with small volume can fill the voids in particleboard, increase the connection between particles and affect the strength of particleboard [7]. The internal bond strength of particleboard with larger sized particles in the core layer is higher than that of particleboard with smaller sized particles in the core layer [8−10]. Thus, in the case of rational use of different particle sizes and factory shavings, we need to redesign the structure of particleboard to meet the requirements of daily use. The typical cross-section feature of particleboard is a layered structure, surface layer is composed of finer and smaller micro particles, and the core layer is composed of coarser and larger particles.

Studies have shown that the high voltage electrostatic field (HVEF) has a positive impact on the surface properties of many materials, and it is applied to the processing and preparation of materials [11−13]. Kilic et al. [14] tested the surface potential of the fiber material under the electric field, and the results showed that the surface free energy of the fiber material increased after the electric field treatment. Qian et al. [15−17] tested the influence of electric field intensity on material bonding under low voltage electric field, and found that the bonding strength increases with increased electric field intensity within a certain range. After electric field treatment, with the increase of treatment degree, the wettability of wood increased, and the adhesive property of the treated wood increased rapidly [18]. The wettability helps to establish a wide range of molecular connections with the wood surface, which is essential for forming strong adhesion at the adhesive-wood interface [19]. When the material is treated by the electric field, the ionization degree in the air increases significantly, resulting in a large number of free charges on the surface of the material, which can significantly improve the surface potential and conductivity of the material [20]. After HVEF treatment, reactions between wood and resin were increased, and electrostatic effects enhanced the bond strength between some water-based adhesives and wood [21]. With the increase of oxidizing groups on the wood surface, the degree of polarization and oxidation on the wood surface increased significantly [22]. So far, the effect of HVEF treatment is limited to the surface of solid wood, and the effect of wood particles is still unclear.

This paper was to study the effect of HVEF treatment on the properties of the particleboard. In the first step, particleboard was manufactured by wood particles of different sizes (A, B, C) and shavings (D), modulus of rupture (MOR), modulus of elasticity (MOE), internal bond (IB) values were tested. In the second step, the MOE of particleboard with different mixture ratios was predicted by using obtained data. In the third step, according to the predicted results, three-layer particleboard was designed. In the fourth step, the effect of HVEF treatment intensities (0 kv, 30 kv, 60 kv) on the important physical properties and mechanical properties of the particleboard was studied.

2 Materials and Method

2.1 Materials

The wood particles are sourced from the factory, and the particles obtained were classified using a vibrating machine and sieves of 8 mesh (2.36 mm), 12 mesh (1.70 mm), 20 mesh (0.850 mm), 30 mesh (0.60 mm). Classified into three sizes (A = –8 + 12 mesh; B = –12 + 20 mesh; C = –20 + 30 mesh). Shavings (D = 3 mm−9 mm) come from a furniture factory. The shavings and particles were dried in a blast drying oven at a drying temperature of 103°C to reduce the moisture content of the wood particles to less than 5%. Urea-formaldehyde (UF) adhesive solid content was 50%, with a formaldehyde/urea (F/U) ratio of 1.4, and viscosity of UF 0.37 Pa.s. Ammonium chloride (0.5%) was added to the resin as a curing agent. No water-repellent chemicals are added to the particleboard.

2.2 High-Voltage Electric Field Treatment

The manufacturing steps of HVEF treated particleboard are shown in Fig. 1. Particleboard is placed between two steel plates inside the hot-press machine. The upper steel plate is connected with the

negative pole of the electric field generator, and the steel plate below the sample is connected with the ground to form a high-voltage electric field between the two steel plates. Place the entire assembly in a hot-press machine and maintain temperature of 160°C. The knob can adjust the voltage on the electrostatic generator. The voltages of 0 kV (10 min), 30 kV (10 min), and 60 kV (10 min) were selected, and the hot pressing and high-voltage electric field treatments were performed simultaneously. After the treatment time was reached, the electric field treatment was stopped, and the entire hot press time was 8 min, and each case was repeated 3 times.

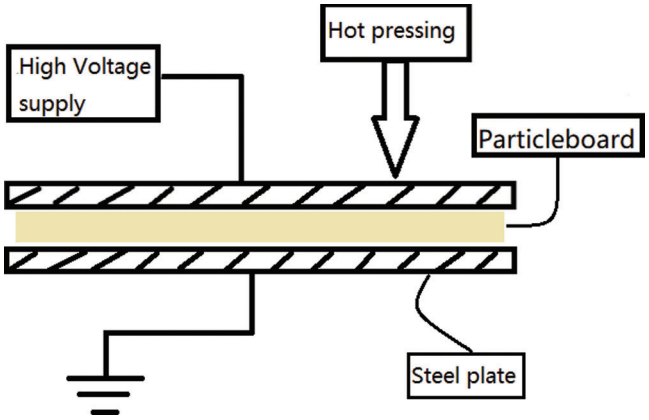

Figure 1: Schematic diagram of hot pressing of particleboard with high voltage electric field

2.3 Uniform Density Particleboard Preparation

The particleboard with dimensions of 400 mm × 400 mm × 10 mm (length × width × height). The particles/shavings were placed in a blender and sprayed with the 12% resin adhesive. Particles with adhesive was taken to a mold with 400 mm × 400 mm × 10 mm. The particles were pre-pressed before hot pressing to consolidate the loose particle. Particleboard were pressed under 2.5 N/mm^2 pressure, at 160°C, for 8 min, the target density of the particleboard design was 700 kg/m^3.

Twelve types of particleboards, with a total of 36 particleboards, were fabricated (Tab. 1). The properties of the composite panels were determined by methods specified in Section 2.5.

2.4 Design and Preparation of Three-Layer Particleboard

The composite modulus assumption for the particleboard specimens is only affected by the physical and mechanical properties of the selected wood, resin, and air. The distribution of elastic constants and strength index parameters along the main axis of the thickness direction depends on the properties of the wood, the properties of the adhesive, and the penetration distribution of the adhesive at the interface form. The specific factors include: 1) The elastic modulus of wood particles, 2) The elastic modulus of resin, 3) The geometry shape of the particles 4) The shear modulus of wood particles. The effects of the vertical density gradient, uniformity, and resin compatibility were not considered in the model. Adhesives are idealized non-void matrix materials, and the stress-strain relationship can be calculated using a continuous function.

Table 1: Uniform density particleboards experimental design

Particleboard types	Particle size (mesh)			Shavings	Intensity (kv)
	-8 + 12	-12 + 20	-20 + 30		
A1	100%				0
B1		100%			0
C1			100%		0
D1				100%	0
A2	100%				30
B2		100%			30
C2			100%		30
D2				100%	30
A3	100%				60
B3		100%			60
C3			100%		60
D3				100%	60

The relationship between the material stiffness Q_{ij} in the principal direction and the elastic constant is:

$$[Q_{ij}] = \begin{bmatrix} Q_{11} & Q_{12} & 0 \\ Q_{12} & Q_{22} & 0 \\ 0 & 0 & Q_{66} \end{bmatrix} = \begin{bmatrix} \frac{E_x}{1-v_{xy}v_{yx}} & \frac{v_{xy}E_y}{1-v_{xy}v_{yx}} & 0 \\ \frac{v_{yx}E_x}{1-v_{yx}v_{xy}} & \frac{E_y}{1-v_{yx}v_{xy}} & 0 \\ 0 & 0 & G_{xy} \end{bmatrix} \tag{1}$$

The volume fraction of each component is of great significance to the application of the micromechanical compound theory. The volume of the resin cannot be measured directly. The volume fraction of the resin is calculated by dividing the volume of the resin by the target volume of each manufactured panel. Assume that the resin does not penetrate into the wood chips.

$$m = m_b + m_a = \rho_b V_b + \rho_a V_a \tag{2}$$

$$v_a = \frac{V_a}{V} \tag{3}$$

$$v_b = \frac{V_b}{V} \tag{4}$$

m is quality of particleboard, V is the volume of the particleboard, v_a is the volume fraction of the adhesive and wood particles in the particleboard, ρ_b, V_b are the density and volume of the wood particles in the particleboard, ρ_a, V_a are the density and volume of the adhesive in the particleboard.

According to the laminated plate theory [23−25] and MALTAB calculation method, the stiffness coefficient matrix D_{ij} is obtained. Thus, the MOE of particleboard can be predicted.

$$D_{ij} = \frac{1}{3}\sum_{k=1}^{N} (Q_{ij})_k \left(z_k^3 - z_{k-1}^3\right) \tag{5}$$

$$E = \frac{12D_{ij}}{t^3} \tag{6}$$

D_{ij} is the bending stiffness matrix of the board; Q_{ij} is the shrinkage stiffness matrix of the particleboard; z_k is the coordinate of the wood particle along the z-axis direction at k; t is the thickness of the particleboards.

After analyzing the results of the uniform density particleboards and the prediction results of MOE, three-layer boards were designed. The Ratio was chosen based on the estimation values of MOE, the surface thickness to a core thickness of 50:50. The ratio of the mixture of A, B, C were 40:40:20. The structural design of the three-layer particleboard is as follows (Fig. 2).

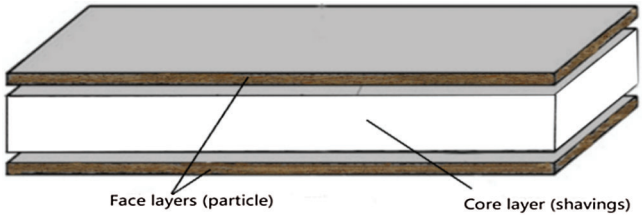

Figure 2: Schematic diagram of three-layer particleboard

Three-layer particleboard manufacturing process, the mixture of A, B, C were placed on the face layers. D were placed in the core layer. The other processes are the same as the uniform particleboard. Three types of HVEF treatment intensities with a total of 9 particleboards were fabricated (Tab. 2).

Table 2: Three-layer particleboards experimental design

Particleboard types	Resign content (%)	Intensity (kv)
M1	12	0
M2	12	30
M3	12	60

2.5 Properties Testing of Composite Materials

All test specimens be conditioned to constant mass in a conditioning room with a relative humidity (RH) of 65% and a temperature of 20°C. After reaching a constant weight, use a circular saw to trim the panel, remove 10 mm from each side, select 5 samples per panel to determine the modulus of rupture (MOR), modulus of elasticity (MOE), according to EN 310 [26]. Eight samples from each particleboard were tested for internal bond (IB), according to EN319 [27]. Both tests were conducted using a computer-controlled electronic universal testing machine with speed of 5 mm/min for bending strength test and 1.5 mm/min for IB test (HD500, Shenzhen Sansi Material Testing Instrument Co., Ltd., China). According to EN 317 standard [28], 8 samples were selected from each board to evaluate the thickness swelling (TS) after 2 h and 24 h, and relative water absorption was tested.

2.6 Density Profile of the Particleboard

Cross-sectional density profiles were measured by X densitometer (EWS, Germany) with scanning speed of 0.5 $mm \cdot s^{-1}$.

2.7 Attenuated Total Reflection Fourier Transform Infrared (ATR-FTIR) Spectroscopy

ATR-FTIR spectroscopic measurements of the particleboards treat with 0 kv, 30 kv and 60 kv were performed using a Fourier transform infrared spectroscopy (FTIR, VERTEX 80V). The spectra were measured on 5 different spots (16 scans per spot) of the coated samples, at a wavelength range from 500 cm^{-1} to 4000 cm^{-1} and a resolution of 2 cm^{-1}.

3 Results and Discussion

3.1 Properties of Uniform Density Particleboard

As shown in Tab. 3, the density of each panel was lower than the preset apparent density (700 kg/m^3), which may be caused by the loss of adhesives and materials during the manufacturing process.

Table 3: Mean values of density, MC, WA and TS of uniform particleboards

Particleboard types	Density (kg/m^3)	MC (%)	TS 24 h (%)	WA 24 h (%)
A1	672(3)	9.69(0.36)	27.24(1.03)	65.14(2.41)
B1	679(5)	9.71(0.27)	24.15(0.88)	69.16(2.57)
C1	675(4)	9.73(0.46)	19.04(0.73)	71.32(2.76)
D1	680(3)	9.65(0.38)	20.68(0.79)	67.56(2.63)
A2	676(4)	9.74(0.47)	25.03(0.87)	58.39(2.04)
B2	669(3)	9.83(0.50)	20.94(0.76)	64.01(2.21)
C2	681(4)	9.68(0.34)	17.56(0.61)	64.90(2.45)
D2	677(3)	9.81(0.40)	18.01(0.68)	59.42(2.19)
A3	680(2)	9.84(0.43)	22.18(0.72)	53.62(1.79)
B3	682(3)	9.91(0.31)	19.11(0.61)	59.83(1.81)
C3	690(1)	9.74(0.55)	14.62(0.46)	60.58(1.92)
D3	688(2)	9.89(0.67)	15.03(0.53)	54.18(1.70)

Note: Numbers in the parenthesis are standard deviations. MC: Moisture Content, WA: Water Absorption, TS: Thickness Swelling.

From Tab. 3, Figs. 3, and 4, the particle size has a significant impact on the mechanical and physical properties of the panel, especially in mechanical properties. Group A displayed the maximum values of MOR and MOE, followed by the values of Group B, Group C has the minimum value. With the increase of the surface of wood particles, the value of IB was increased. The panel manufactured by particle D has the highest IB value, while the panel manufactured by particle C has the lowest IB value. The larger surface contact area leads to better bonding, which may be the reason for the better strength characteristics of such panels. It was observed that the mean TS value (24 h) decreased with the increase of the proportion of smaller-size particles in the panel. Compared with other groups, the dimensional stabilities of panel manufactured by Group C is higher, and the thickness swelling within 24 h is lower. The IB of panel made from larger/longer sized particles in the core layer was significantly higher than the panel with smaller sized particles in core layer. Therefore, particles D were used as the core layer of three-layer particleboard. A and B are used as the surface of three-layer particleboard because of the

higher MOR and MOE. In addition, due the small size of particles C, particles C are added to the production panel to fill the void spaces in the panel, it can improve the surface characteristics of the panel, and make panel surface smooth.

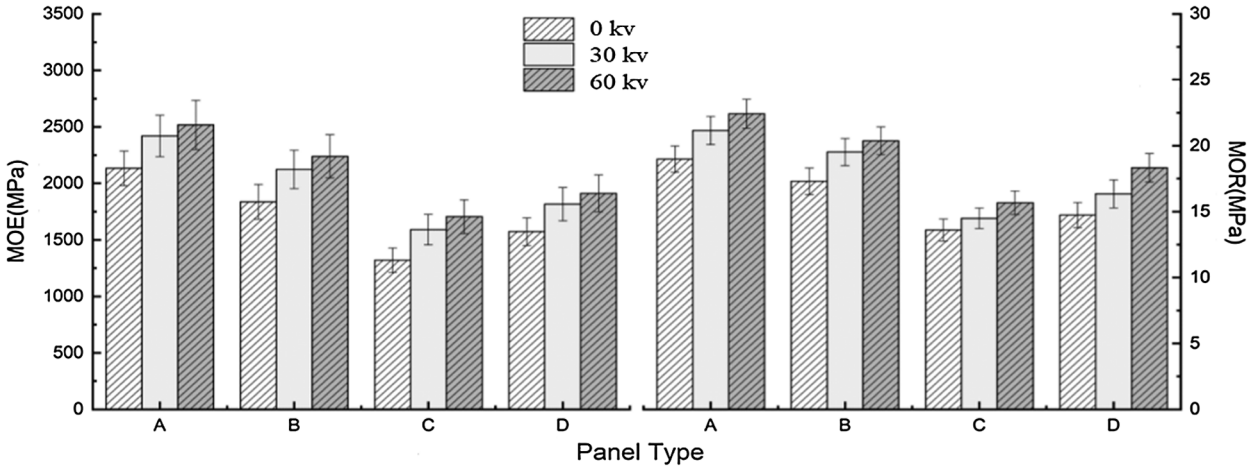

Figure 3: MOE and MOR of particleboards

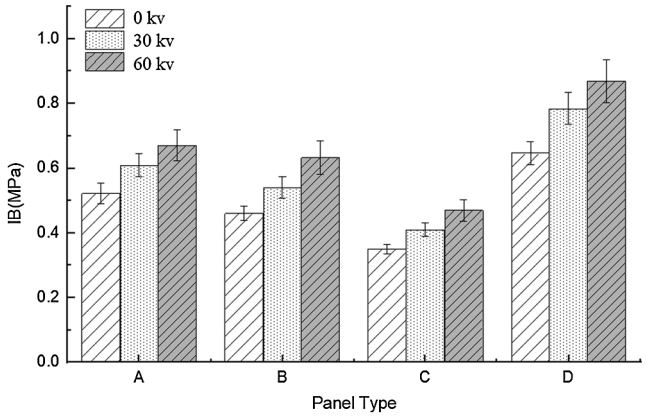

Figure 4: IB of particleboards

3.2 Particleboard Design and Model Verification

In research by Bodig and Jayne, wood composites are considered to be isotropic [29]. In the particleboard model, the Poisson's ratio uses a nominal constant value of 0.30 [30]. For isotropic materials $E_x = E_y$. The elastic constant of the urea-formaldehyde resin is obtained from the literature [31]. The spring constant of air is set to zero (no contribution to performance). The interlayer shear modulus is compared with the previous research value [32].

The relationship between the surface thickness and MOE was calculated by using the laminate theory and MATLAB calculation method. As shown in Fig. 5, when the face layer thickness was less than 2.5, the MOE values increase rapidly, and when the surface thickness was greater than 2.5, the MOE values increase little. Considering the physical properties and mechanical properties of particleboard, we choose the ratio of surface thickness to a core thickness of 50% to 50%.

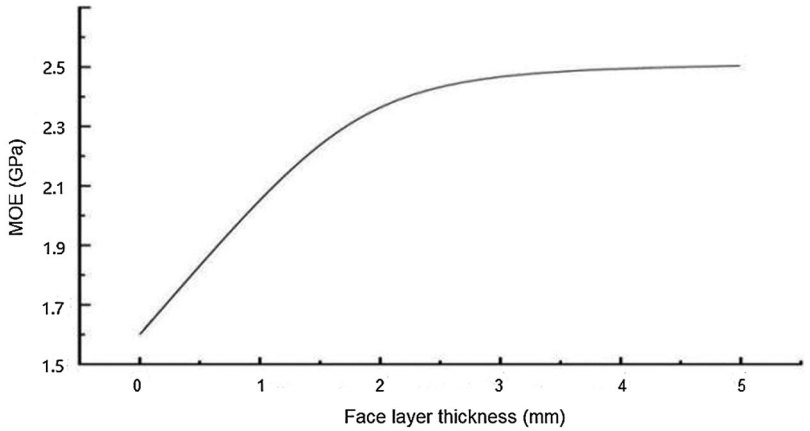

Figure 5: Relationship between the surface thickness of particleboards and the predicted value of MOE

Under the HVEF treatment, the elastic constants of the face layer, core layer, and urea-formaldehyde resin are shown in Tab. 4.

Table 4: Basic engineering properties of structural particleboards

	E_x	E_y	G_{xy}	V_{xy}
Face layer	2.4	2.4	0.29	0.30
Core layer	1.8	1.8	0.45	0.30
UF	7.8	7.8	7.3	0.44

MOE values of particleboard were predicted according to MTALAB, the predicted value was compared with the measured value, as shown in Tab. 5. The maximum relative errors of mechanical properties of particleboard are all less than 20% (correlation coefficient $R^2 > 80\%$, at the level of 0.01) regardless of whether the samples were treated by high voltage electric field or not.

Table 5: Measured and predicted values

Particleboard types	MOE value (N/mm^2)		Relative error
	Experimental results	Modeling results	
M1	2315	2037	13.7%
M2	2542	2315	14.9%
M3	2787	2386	16.8%

Besides, the estimation values of MOE and MOR are lower than the measured values. This change is due to not considering the particle board in the preparation of thermal stress and humidity. These factors can affect particleboard interface performance and mechanical performance [33]. At the same time, the uniformity of the bonding interface is not an ideal material. Under shear loading, particleboards interface is easy to appear some concentrated stress, which affects the interface stiffness and strength distribution.

3.3 Properties of Three-Layer Particleboard

The thickness swelling and water absorption of the panels are listed in Tab. 6. TS was ranging from 15% to 17.9%. The results show that the TS (24 h) and WA (24 h) of the particleboards decreased when the HVEF treatment intensities increased. The average TS values of the boards decreased to 15.0% under HVEF treatment (60 kv), indicating that increasing electrostatic intensity contributed to the improvement of bonding performance of the particleboard. This result may be related to the polarization process of adhesion bonds in HVEF and a better aggregation performance of adhesive on particles surface [34].

Table 6: The properties test of the three-layer particleboards

Particle-board types	Density (kg/m^3)	MC (%)	MOR (N/mm^2)	MOE (N/mm^2)	IB (N/mm^2)	TS 2hrs (%)	TS 24hrs (%)	WA 2hrs (%)	WA 24hrs (%)
M1	683(3)	9.70 (0.41)	19.40 (0.40)	2265 (137)	0.68 (0.03)	14.7 (0.52)	17.9 (0.62)	61.4 (2.13)	65.5 (2.32)
M2	691(2)	9.87 (0.37)	21.72 (0.46)	2542 (132)	0.78 (0.04)	13.6 (0.48)	16.3 (0.58)	53.9 (1.79)	57.6 (2.06)
M3	693(4)	9.92 (0.42)	23.61 (0.43)	2787 (142)	0.86 (0.04)	12.5 (0.41)	15.0 (0.52)	47.7 (1.61)	51.2 (1.77)

Note: Numbers in the parenthesis are standard deviations.

Tab. 6 illustrates MOE, MOR, and IB values of the panels manufactured with different HVEF treatments, respectively. The improvement of mechanical properties was dependent on HVEF treatment intensity. The MOE, MOR, and IB values of HVEF treatment (60 kv) samples were 2787 N/mm^2, 23.61 N/mm^2, and 0.86 N/mm^2, respectively, which were 22.7%, 21.6%, and 26.5% higher than those of the particleboard without HVEF treatment. The explanation for the increased mechanical properties of the panels is associated with the more cross-linked UF resin. Through the HVEF treatment, the oxidation of the highly hydrophobic surface layer of the neutral part of the wood extract reduced their hydrophobicity [35]. The wettability of wood particles was improved significantly in the HVEF treatment, which led to the increase of wood surface polarity and the wood particle adhesion to water-based adhesives. HVEF treatment increases the surface energy, especially in polar component. With the increase of electric field intensity, electrons collide with the chemical group of water and oxygen molecules in the air are excited, to form many broken chemical bonds, such as -OH and -CHO [36]. More free chemical bonds and ions act on the material surface. The fractured oxygen-containing group reacts with the group on the material surface, significantly increasing the degree of polarization and oxidation on the material surface [37].

3.4 Density Profile of the Particleboards

Tab. 7 shows the density measurement results of particleboard, the face layer density of particleboard is higher than that of the core layer (Fig. 6).

Table 7: Density profile determination with results

Particleboard types	Mean maximum density (lower face layer) (kg/m^3)	Mean minimal density (kg/m^3)	Mean maximum density (upper face layer) (kg/m^3)	Mean panel Density (kg/m^3)
M1	737	639	741	683
M2	761	634	755	691
M3	782	628	769	693

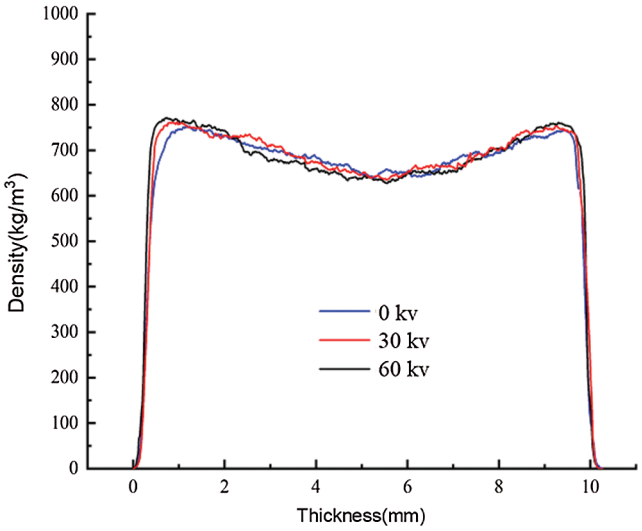

Figure 6: Vertical density profiles of three-layer particleboards with different HVEF treatment intensities

For three-layer particleboard, the surface layer of the particleboard bears most of the load in the bending process, the higher the density of the surface layer, the better the mechanical properties, especially the bending properties [38]. The increase in electric field intensity leads to increased surface density, with a higher peak closer to the surface. The maximum density increment under different intensity is: 3.3% (30 kV), 6.1% (60 kV). This may be attributed to the increase of HVEF treatment voltages, the improvement of aggregation performance, and the surface layer is more compact, leading to a great density difference between the surface and core layers.

3.5 ATR-FTIR Analysis

The effect of high voltage electric field on chemical groups on the surface of three-layer particleboard was characterized by FTIR, and the results are shown in Fig. 7. The main functional groups on the material surface were compared under different HVEF treatment, the peak value of 3334 cm^{-1} was due to the tensile vibration of hydroxyl band, which significantly increased compared with the control group. The 1731 cm^{-1} presented a peak which is related to axial stretching of carbonyl groups (C=O) in carboxylic acid groups. The bands of IR spectra at 1508 cm^{-1} were attributed to the aromatic ring vibrations of the guaiacyl present in lignin [38]. The peak at 1250 cm^{-1}, indicating stretching the C-O bond of -O-(C=O)-. Under HVEF treatment, the increase of electrons on wood surface, the fracture and polarization of chemical bands lead to the increase of these bands. In addition, the C-O band of 830 cm^{-1} is the tensile strength of hydroxymethyl group, which shows an increasing trend under HVEF treatment. Steele [39] showed that the increase of C-O functional groups in the glue solution was conducive to improving the cross-linking reaction between the glue solution and wood chemical groups. Under HVEF treatment, the higher intensities of these bands indicates that HVEF treatment can significantly increase the content of free radicals and oxygen-containing groups on the surface of wood particles, increase the degree of polarization, and provide more reaction sites for its reaction with other polymers [40]. Moreover, under the condition of 60 kV treatment, the intensity of each characteristic peak is increased compared with that of untreated [41].

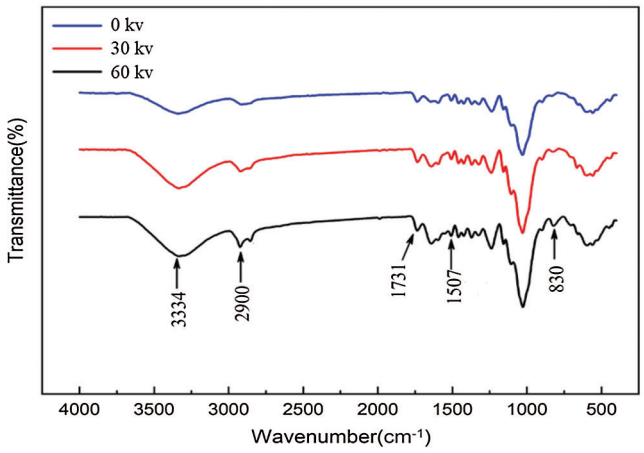

Figure 7: ATR FTIR spectra of control and HVEF treated samples

4 Conclusion

In this study, the elastic modulus was predicted by using MATLAB software. The accuracy of prediction is more than 80%. According to the prediction results, three-layer particleboards are successfully manufactured from wood particles and shavings by optimizing the technological parameters, which proved to be a promising method. Properties of particleboard were evaluated. With the increase of electric field intensity, the properties of particleboard were improved, especially, and IB increased most significantly. The IB improvement was 25.6% under HVEF treatment (60 KV). This effect is attributed to the increase of polarization and crosslinking degree of UF resin and the preferable wettability of wood particles. Under HVEF treatment (60 kV), the MOR, MOE, and IB of three-layer particleboard were 23.61 N/mm^2, 2787.09 N/mm^2, and 0.86 N/mm^2. With HVEF treatment intensities increased, the face layers were more compacted. The properties of three-layer particleboard meet the requirements of MOE, MOR, and IB in EN312 standard.

Acknowledgement: All authors contributed equally to this work.

Funding Statement: The Authors acknowledge funding support by the National Key R&D Program of China (2017YFC0703501). The authors wish to acknowledge the National Natural Science Foundation of China (Grant No. 32071700).

Conflicts of Interest: The authors declare that they have no conflicts of interest to report regarding the present study.

References

1. Pelaez-Samaniego, M. R., Yadama, V., Lowell, E., Espinoza-Herrera, R. (2013). A review of wood thermal pretreatments to improve wood composite properties. *Wood Science and Technology, 47(6),* 1285–1319. DOI 10.1007/s00226-013-0574-3.
2. Aisien, F., Amenaghawon, A., Bienose, K. (2015). Particle boards produced from cassava stalks: Evaluation of physical and mechanical properties. *South African Journal of Science, 111(1–4)*.
3. Simal Alves, L., da Silva, S. A. M., Maximiliano, D. A. A., Varanda, L. D., Christofóro, A. L. et al. (2014). Particleboard produced with sawmill waste of different wood species. *Advanced Materials Research, 884−885,* 689–693. DOI 10.4028/www.scientific.net/AMR.884-885.689.
4. Altgen, D., Avramidis, G., Mai, C. (2016). The effect of air plasma treatment at atmospheric pressure on thermally modified wood surfaces. *Wood Science and Technology, 50(6),* 1–15.

5. Frybort, S., Mauritz, R., Teischinger, A., Ulric, M. (2008). Cement bonded composites–A mechanical review. *Bioresources, 3(2),* 602–626.
6. Nishimura, T., Amin, J., Ansell, M. P. (2004). Image analysis and bending properties of model OSB panels as a function of strand distribution, shape and size. *Wood Science and Technology, 38(4),* 297–309. DOI 10.1007/s00226-003-0219-z.
7. Moslemi, A. A. (1974). *Particleboard*. Carbondale: Volume 1: Materials, pp. 244. Southern Illinois University Press.
8. Jamaludin, K., Jalil, A., Jalaludin, H., Zaidon, A. (2001). Properties of particleboard manufactured from commonly utilized Malaysian bamboo (Gigantochloa scortechinii). *Pertanika Journal of Tropical Agricultural Science, 24(2),* 151–157.
9. Lee, O. L., Paridah, M. T. (2003). Effect of fine particle content on the properties of five layered oriented strands board (OSB). *XII World Forestry Congress,* Quebee City, Canada.
10. Rackwitz, G. (1963). Influence of chip dimensions on some properties of wood particleboard. *Holz als Roh-und Werkstoff, 21(6),* 200–209. DOI 10.1007/BF02609724.
11. He, Q., Zhan, T., Ju, Z., Zhang, H., Hong, L. et al. (2019). Influence of high voltage electrostatic field (HVEF) on bonding characteristics of masson (pinus massoniana lamb.) veneer composites. *European Journal of Wood and Wood Products, 77(1),* 105–114. DOI 10.1007/s00107-018-1360-6.
12. Zheng, Y., Zeng, Y. (2014). Electric field analysis of spinneret design for multihole electrospinning system. *Journal of Materials Science, 49(5),* 1964–1972. DOI 10.1007/s10853-013-7882-8.
13. Kemp, B. A., Nikolayev, I., Sheppard, C. J. (2016). Coupled electrostatic and material surface stresses yield anomalous particle interactions and deformation. *Journal of Applied Physics, 119(14),* 145105. DOI 10.1063/1.4946034.
14. Kilic, A., Shim, E., Pourdeyhimi, B. (2015). Measuring electrostatic properties of fibrous materials: A review and a modified surface potential decay technique. *Journal of Electrostatics, 74,* 21–26. DOI 10.1016/j.elstat.2014.12.007.
15. Qian, J., Zhang, W., Jin, Y., Li, Y., Feng, Z. (1999). The study on the influence of electric field on bonding properties of poplar composites. *Wood Science and Technology of Zhejiang Forestry University, 13,* 7–9.
16. Qian, J., Jin, Y., Yu, Y., Yan, J., Zhang, H. (2002). Effects of potential difference of setting plate on Sakhu-bonding. *Wood Science and Technology of Zhejiang Forestry University, 26,* 41–43.
17. Qian, J., Jin, Y., Shen, Z., Yu, Y., Lou, Y. (2005). Effect of intensity and work time of electric field onmoisture gradient of Pinus massoniana wood. *Wood Science and Technology of Zhejiang Forestry University, 22,* 193–197.
18. Sakata, I., Morita, M., Tsuruta, N., Morita, K. (1993). Activation of wood surface by corona treatment to improve adhesive bonding. *Journal of Applied Polymer Science, 49(7),* 1251–1258. DOI 10.1002/app.1993.070490714.
19. Frihart, C. H. (2005). Wood adhesion and adhesive. In: Rowel, R. M. (eds.), *Handbook of wood chemistry and wood composites,* pp. 230–238. Boca Raton, FL: CRC Press.
20. Jankowiak, A., Collardey, F., Blanchart, P. (2005). Electrical behaviour at high voltage on surface of *Si*C-β′-SiAlON ceramic composites. *Journal of the European Ceramic Society, 25(1),* 13–18. DOI 10.1016/j.jeurceramsoc.2004.02.003.
21. Zamilova, A. F., Galikhanov, M. F. (2016). Influence of polarization of the walnut plywood in the process of preparation on its water and moisture absorption. *Physics, Technologies and Innovation (PTI-2016): Proceedings of the III International Young Researchers' Conference,* AIP Publishing LLC.
22. He, Q., Zhan, T. Y., Zhang, H. Y., Ju, Z. H., Hong, L. et al. (2019). Robust and durable bonding performance of bamboo induced by high voltage electrostatic field treatment. *Industrial Crops and Products, 137(6),* 149–156. DOI 10.1016/j.indcrop.2019.05.010.
23. Lu, X., Pizzi, A. (1998). Interior MDI/pine tannin plywood adhesives without formaldehyde. *Holz als Roh-und Werkstoff, 56(1),* 78. DOI 10.1007/s001070050267.
24. Lu, X., Chen, Y. C., Chen, Y. (2002). Prediction model of along-grain elastic modulus of fast-growing poplar veneer. *Journal of Nanjing Forestry University, (3),* 9–13.

25. Zhang, H., Luo, H., Lu, X. (2014). The analysis of compression strength of hennon bamboo reinforced extruded particleboard. *Journal of Forestry Engineering, 28(6),* 72–74.
26. EN 310 (1993). *Wood-based panels, determination of modulus of elasticity in bending and bending strength,* vol. 13. Brussels, Belgium: European Committee for Standardization.
27. EN 319 (1993). *Particleboards and fiberboards, determination of tensile strength perpendicular to plane of the board*. Brussels, Belgium: European Committee for Standardization.
28. EN 317 (1993). *Particleboards and fiberboards, determination of swelling in thickness after immersion,* vol. 12. Brussels, Belgium: European Committee for Standardization.
29. Bodig, J., Jayne, B. A. (1993). *Mechanics of wood composites,* pp. 712. Malabor, FL: Krieger Publishing Company, 712.
30. Bulleit, W. M. (1985). Elastic analysis of surface reinforced particleboard. *Forest Products Journal, 35(5),* 61–68.
31. Zhang, L. L. (2009). *Bamboo fiber composites microstructure design, preparation and properties research (Ph.D. Thesis)*. Nanjing Forestry University.
32. Lehmann, W. F., Geimer, R. L. (1974). Properties of structural particleboards from Douglas-fir forest residues. *Forest Products Journal, 24,* 17–25.
33. Thoemen, H., Haselein, C. R., Humphrey, P. E. (2006). Modeling the physical processes relevant during hot pressing of wood-based composites. Part II. Rheology. *Holz als Roh-und Werkstoff, 64(2),* 125–133. DOI 10.1007/s00107-005-0032-5.
34. He, Q., Zhan, T., Zhang, H., Ju, Z., Dai, C. et al. (2018). The effect of high voltage electrostatic field (HVEF) treatment on bonding interphase characteristics among different wood sections of Masson pine (Pinus massoniana Lamb.). *Holzforschung, 72(7),* 557–565. DOI 10.1515/hf-2017-0168.
35. Hon, D., Feist, W. C. (1981). Free radical formation in wood: The role of water. *Wood Science, 14(1),* 41–48.
36. Ghazian, O., Adamiak, K., Castle, G. S. P., Higashiyama, Y. (2014). Oscillation, pseudo-rotation and coalescence of sessile droplets in a rotating electric field. *Colloids and Surfaces A: Physicochemical and Engineering Aspects, 441,* 346–353. DOI 10.1016/j.colsurfa.2013.09.017.
37. Broughton, J., Cruz, H., Winfield, P. (2009). Activation of timber surfaces by flame and corona treatments to improve adhesion. *International Journal of Adhesion and Adhesives, 29(2),* 167–172. DOI 10.1016/j.ijadhadh.2008.03.003.
38. Wong, E. D., Zhang, M., Wang, Q., Kawai, S. (1998). Effects of mat moisture and press closing speed on the formation of density profile and properties of particleboard. *Journal of Wood Science, 44(4),* 287–295. DOI 10.1007/BF00581309.
39. Herbert, H. L. (1971). Lignins: Occurrence, formation, structure and reactions. In: Sarkanen, K. U., Ludwig, C. H. (eds.), *Infrared spectra,* pp. 267–297. New York: John Wiley and Sons.
40. Steele, R. (1960). Catalysis of the reaction of urea–formaldehyde precondensates on cellulose. *Journal of Applied Polymer Science, 4(10),* 45–54. DOI 10.1002/app.1960.070041007.
41. Truss, R. W., Wood, B., Rasch, R. (2016). Quantitative surface analysis of hemp fibers using XPS, conventional and low voltage in-lens SEM. *Journal of Applied Polymer Science, 133(8),* DOI 10.1002/app.43023.